International Journal of Current Bio-Medical Engineering (IJCBE)
Volume 1, Issue 1, September – October (2023)

RESEARCH ARTICLE

BRAIN ANEURYSM DETECTION VIA FIREFLY OPTIMIZED SPIKING NEURAL NETWORK

A. Jegatheesh[1, *], N. Kopperundevi[2] and M. Anlin Sahaya Infant Tinu[3]

[1]Assistant Professor, Department of Biomedical Engineering, SRM Institute of Science and Technology, Ramapuram Campus, Chennai, Tamil Nadu, India.

[2]Assistant Professor SG-2, School of Computer Science and Engineering, Vellore Institute of Technology, Vellore, Tamil Nadu, India.

[3]Research Scholar, Department of Electronics and Communication Engineering, Anna University, Chennai, Tamil Nadu, India.

[*]*Corresponding e-mail:abjegatheesh@gmail.com*

Abstract – Aneurysms in the brain occur often; the frequency is around 4%. The mass effect is mostly responsible for the symptoms of unruptured aneurysms. The actual risk arises if the aneurysm bursts and results in a subarachnoid haemorrhage, though. The majority of aneurysms are asymptomatic and do not burst, although even minor aneurysms can do so due to the unpredictable growth of aneurysms. Imaging methods including intra-arterial digital subtraction angiography, computed tomography angiography, and magnetic resonance angiography are used to diagnose and track intracranial aneurysms. In this paper, a deep learning approach is proposed to detect and classify the brain aneurysm. Initially, the MRI images are skull stripped and the images augmented and reduce the noise using Kalman filter in the pre-process phase. The segmentation can be done by the firefly optimization algorithm. The segment nodules are classified into three classes by using the spiking neural network. The proposed model achieves the highest level of classification accuracy, which is 99.80%. As a result, when compared to other models currently in use, classification using BSF yields results that are much higher in efficiency and accuracy.

Keywords *– Brain aneurysm, firefly optimization algorithm, Kalman filter, spiking neural network.*

1. INTRODUCTION

A brain aneurysm is a dangerously enlarged, blood-filled region of a weak or thinning blood vessel in the brain. A larger aneurysm increases the risk of rupture and subarachnoid haemorrhage (SAH) by compressing the surrounding neurons and brain tissue. The possibility of such a rupture is affected by the aneurysm size and shape [1]. Cutting the aneurysm neck is a viable surgical technique to stop rupture. Therefore, knowing the shape of a cerebral aneurysm is crucial for both identifying cerebral aneurysms and determining the position and posture of the required clips during diagnostic testing [2].

Some patients did not show cerebral bleeding despite having rupture aneurysms. On the other hand, it can be hard to identify which aneurysm ruptures in patients with numerous aneurysms, even though there is cerebral bleeding. Determining the condition of brain aneurysms accurately is therefore crucial for medical care and prognosis assessment [3,4]. While the treatment of aneurysms that have not ruptured is uncertain ruptured aneurysms require immediate surgery. Some unruptured aneurysms may never show symptoms [5], and problems might result from intravascular or microsurgical treatment. [6].

Brain aneurysms may be detected non-invasively, accurately, and reliably using computed tomography angiography (CTA) [7]. CTA demonstrated that a number of morphological characteristics, including diameter, aneurysm length, height, breadth, surface area, volume, etc., were related to aneurysm rupture when comparing the morphologies of ruptured and unruptured aneurysms. Other studies have demonstrated the value of using CTA images to classify ruptured and unruptured cerebral aneurysms using radiomics [8]. The following are the contributions of this research:

- The dataset used in this study, which includes training pictures of brain aneurysms, contains brain MRI scans.
- From the MRI images the skull stripped and the input images are augmented. By using this Kalman filter pre-process these MRI images to reducing the noise.
- The segmentation process can be done by using the Firefly optimization algorithm and the brain nodules are segment.

- The segmented brain nodules are taken as the input of the classification phase. That inputs are classified into three classes by using the spiking neural network such as Saccular Aneurysm (SA), Mycotic aneurysm (MA) and fusiform aneurysm (FA).

The remaining five portions of this paper were organised as follows. The literature review is presented in Section 2, the suggested approach for treating brain aneurysms using a spiking neural network and Section 3 introduces the firefly optimisation algorithm (BSF), Section 4 presents the findings and discussion, and Section 5 offers a conclusion.

2. RELATED WORK

Recently the researchers used a variety of deep learning and machine learning techniques mainly to improve the accuracy of detecting brain aneurysm from the MRI images. In this section, a few of those methods are studied shortly discussed.

In 2023 Xie, Y., et al., [9] employed a 3D convolutional neural network (CNN) encoder that automatically extracts complex hidden information. The best characteristics that are particularly relevant to the fracture risk data are found using the LASSO regression method, and a support vector machine (SVM) is employed to make the final fracture risk prediction. According to test findings, our classification approach can produce accuracy and AUC values of 89.78% and 89.09%, respectively.

In 2023 Regaya, Y., et al., [10] presented a technique for segmenting cerebral aneurysms in two dimensions using statistical and multiresolution methods. HMRF-EM (Expectation maximization in a hidden Markov random field) segments images based on spatial context restrictions while Contourlet Transform (CT) collects image features. The accuracy was attained 99.72%.

In 2023 Fujimura, S., et al., [11] created a machine learning model (MLM), In order to predict the ideal size and length of the first coil by gathering data on patients and aneurysms that had previously had successful coil embolization treatment. The accuracy rate of the prediction of size and length is 86.3% and 83.4% respectively.

In 2023 Ishihara, M.,et al., [12] evaluated the capability of convolutional neural network (CNN) scores features to distinguish between infundibular dilatation (ID) and an unruptured aneurysm (UAN). Using magnetic resonance angiography, we apply clinically available deep learning-based computer-aided diagnostic tools to identify unruptured aneurysms (UANs). Overall, the accuracy is 83.2%, specificity is 82.6%, and sensitivity is 89.0%.

In 2023 Niemann, A., et al.,[13] suggested a pipeline for analyzing cerebral aneurysms that includes automatic center line and outlet recognition, Segmenting networks using deep learning (MeshCNN) and generating semantic angiograms automatically. Morphological analysis with automatic injury status categorization and semantic angiography. The 3D surface models may also be used to classify rupture states, which has an accuracy of 83.3%.

In 2023 Li, X., et al.,[14] proposed best machine learning approach to investigate the risk variables for Haemorrhagic transformation (HT) after Acute cerebral infarction (ACI) and create a model that can accurately assess both the likelihood of HT occurrence, it examines various machine learning methods. The HT risk prediction model developed by the XgBoost algorithm performed best, with an accuracy rate of 95%.

In 2022 Lei, X., et al., [15], A network based on the three-dimensional (3D) U-Net model was constructed, and the network was fed the collected image data in order to perform the automatic localization and segmentation of the aneurysm. In order to find and pinpoint potential aneurysm locations, the 3D convolutional neural network (CNN) network can extract the aneurysm blood vessels. The degree of accuracy is 97.19%.

Several machine learning and deep learning algorithms were developed from these related efforts with the goal of classifying brain aneurysms. By categorising brain aneurysms into three classes—saccular aneurysm, mycotic aneurysm, and fusiform aneurysm—the proposed BSF framework also aims to increase classification accuracy. The deep learning-based Firefly optimization algorithm is used for segmentation, in which spiking neural network employed for classifying the MRI images into three different classes with high accuracy to early detection of brain aneurysm.

3. PROPOSED MODELLING

In this section, we proposed a deep learning-based framework for classifying brain aneurysm into three classes from the MRI brain images. The figure shows the three steps of the proposed system. The Kalman filter is used to first eliminate the noise artefacts. Using the firefly optimisation approach, the pre-processed MRI images are used as an input for segmentation. Based on these segment nodules, a spiking neural network classifies the pictures as having saccular, mycotic, or fusiform aneurysms. The suggested BSF model's entire workflow is depicted in Figure 1.

3.1. Dataset

The brain MRI images were acquired from IntaA datasets. 103 Reconstructing the patient's scanned 2D MRA images yields 3D models of all the patient brain vessels. 1,909 vessel segments, including 215 aneurysm segments for diagnosis and 1,694 healthy vascular segments, are created automatically from the entire model. A medical expert manually splits and annotates 116 aneurysm segments. The requirement for preoperative examination determines the size of each aneurysm section.

3.2. Data Pre-processing Phase

In this paper the MRI images are preprocessing by using the Kalman filter for reduce the noise. The Kalman filter effectively manages uncertainty brought on by irregular external influences and noisy sensor data. Using

the projected system state and a weighted average, the Kalman filter generates an estimate of the system state from the average of fresh measurements. Equations 1 to 6 display the Kalman filter equations for the prediction steps.

$$\hat{a}_{\bar{k}} = L\hat{a}_{\bar{k}} + Mu_k + w_k \quad (1)$$

$$A_k = \mathrm{L}LA_{k-1} + L^T + B \quad (2)$$

$$K_k = A_{\bar{k}}H^T(DA_{\bar{k}}D^T + C)^{-1} \quad (3)$$

where, $\hat{a}_{\bar{k}}$ is a vector prediction, $\hat{A}_k$ is the predictive covariance matrix and K_k is kalman gain. Next predictions are updated with measurementsz_k

$$\hat{a}_{\bar{k}} = \hat{a}_{\bar{k}} + K_k(z_k - D\hat{a}_{\bar{k}}) \quad (4)$$

$$z_k = \mathrm{D}\hat{a}_{\bar{k}} + v_k \quad (5)$$

Then the error covariance is update

$$A_k = (N - K_kD)A_k \quad (6)$$

Predictions about the upcoming condition will be made using the updated state variable. As many times as necessary for the needed time discretization, these processes will be repeated.

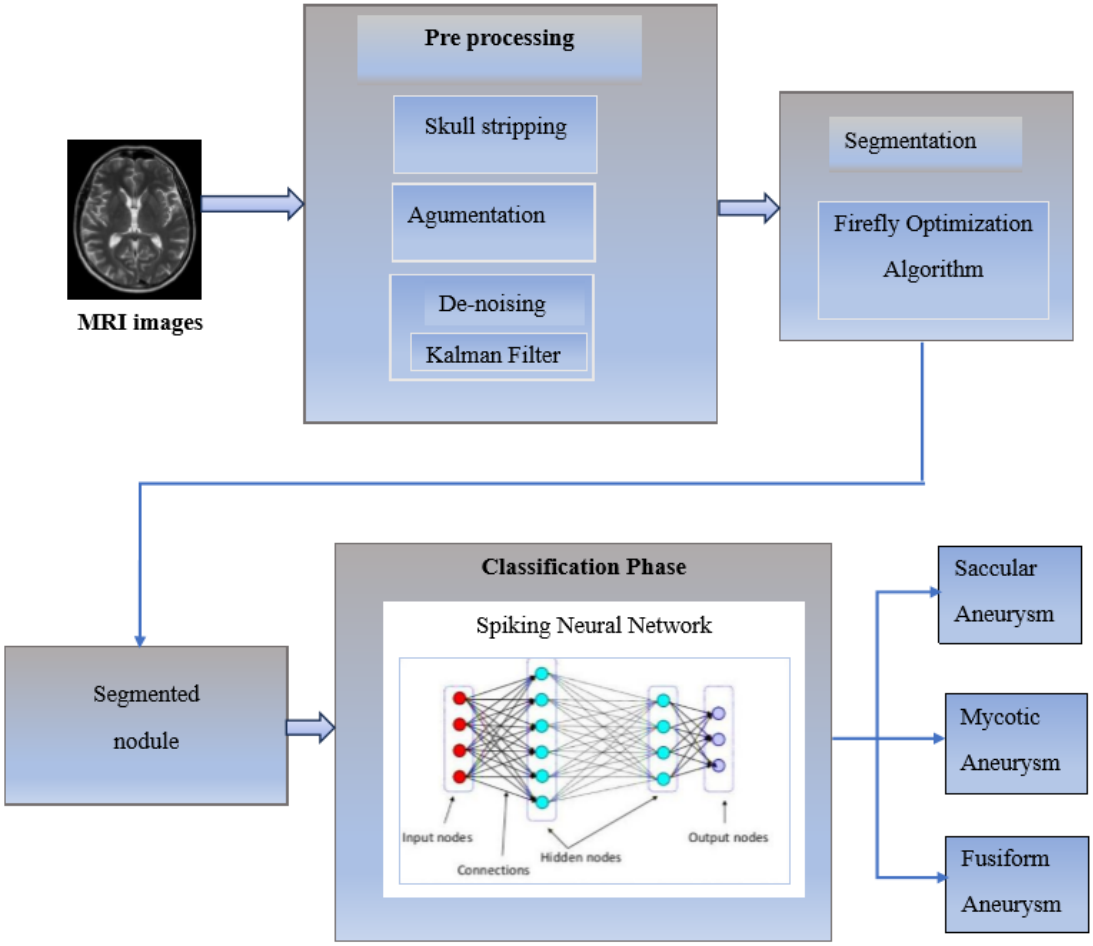

Figure 1. Proposed method working architecture

3.3. Segmentation Phase

The segmentation done by using the Firefly Optimization algorithm which affected by Firefly flickering behaviour. The patch is ultimately located using the algorithm left-to-right and top-to-bottom searches for the best matching patch. However, a lot of work and errors happen when there are numerous candidate fixes. To discover the best matching patch, a Firefly optimization technique was developed. Numerous applications have used the Firefly Optimisation technique to tackle a range of optimisation problems. Constrained, multi-criteria, and discrete optimization issues have all been addressed by Firefly Optimization algorithm.

Using the Firefly method, aneurysm affected portions are accurately identified in images, segmentation and class selection are optimized to recover the true aneurysm affected portion. The Firefly algorithm chooses appropriate features by examining the texture of image pixels. The Firefly algorithm processes for optimizing image segmentation are shown in Figure 2.

Image segmentation is optimized by the Firefly algorithm. Make a starting population of fireflies, specify the parameters for attraction, absorption, and selection, then make a new population and figure out the fitness function. The satisfaction criteria are examined following a number

of iterations, and if they are met, the preceding step or exit is chosen.

This algorithm development considers differences in brightness or light intensity in addition to the notion of attractiveness. A form of adaptive function is used to represent and quantify firefly brightness, with varied light intensities for various light sources. The intensity of the light affects brightness, which determines attractiveness. The following formula is used to determine each firefly level of attraction (7).

$$\beta(t) = \beta_0 e^{-\gamma t^2} \quad (7)$$

where $\beta_0$denotes the attractive force at distance (t) = 0, which in mathematical calculations can be treated as 1. The height of light absorption is denoted by the symbol. T represents the separation of two fireflies, i and j, located at various locations.

Figure 2. Firefly Algorithm flow diagram for optimization of image segmentation

Fireflies frequently change their locations. This shows that firefly' attraction to one another may be influenced by distance. As a result, the well-known Euclidean distance rule is used to calculate the distance between any two fireflies, i and j:

$$t_{ij} = |a_i - a_j| = \sqrt{\sum_{k=1}^{d} (a_{i,k} - a_{j,k})^2} \quad (8)$$

where d is the problem's size and a_(i,j) is the position of firefly i's k-th component. Assume that firefly i and firefly j are drawn to one another and move in that direction after determining the distance between the two fireflies. Equation (9) governs this kind of motion and is denoted by

$$a_i^{n+1} = a_i^n + \beta_0 e^{-(\gamma t_{ij}^2)} * (a_j^n - a_i^n) + \alpha * (rand - \tfrac{1}{2}) \quad (9)$$

where n represents the number of iterations, coefficient the size of the random walk, and rand a random number generator that produces numbers between [0, 1]. After three words are weighed, low intensity fireflies turn into high intensity fireflies. The first word is the current position of the low brightness firefly. The second term is the movement by the attraction coefficient towards the firefly with higher brightness. In order to determine the final term, a random number generator is multiplied by a sort of random walk.

3.4. Classification Phase

The Spiki Neural Network classify the brain aneurysm into three different classes such as saccular aneurysm, Mycotic aneurysm and fusiform aneurysm. In a genuine neuron, the biophysical processes of potential creation on the neuron membrane are represented by differential equations that control impulse transmission. One of the most popular mathematical models for precisely simulating the biological function of the neuron is a leaky integrate-and-fire (LIF) neuron.

According to this model, the input L(t) is a voltage increase that updates the hidden state (membrane potential), M(t), which in turn causes spikes to appear in the output P(t). The membrane potential following the spike trigger is represented by N (t). These equations can be used to explain its behaviour.

$$M(t) = f\,(N\,(t-1), L(t)) \quad (10)$$

$$P(t) = g(M(t) - Nthreshold) \quad (11)$$

$$= \theta(L(t) - Nthreshold)$$

$$N\,(t) = L(t)\,(1 - P(t)) + NresetP(t) \quad (12)$$

Nthreshold is the threshold for spike firing, L(t) is the input to the neuron at timestep t, Nreset is the potential to which the neuron returns following the spike, and so on. The neuron's state update equation is denoted by the notation f (N (t 1), L(t)). The update function utilised for the LIF neuron is as follows, where is a membrane time constant:

$$M(t) = f\,(N\,(t-1), L(t)) \quad (13)$$

$$= N\,(t-1) - 1\,\tau\,((N\,(t-1) + Nreset) + L(t))$$

The Heaviside step function θ(x), which has the following definition, is utilised for the spike generating function g(t):

$$\theta(x) = \begin{cases} 1, for\ x \geq 0 \\ 0, for\ x < 0 \end{cases} \quad (14)$$

4. RESULTS AND DISCUSSIONS

The deep learning toolbox MATLAB 2019b was used to implement the experimental design of this work. The three kinds of brain aneurysms were classified using MRI images from the IntrA dataset in this outcome analysis. Utilising the particular characteristics, the suggested BSF approach's effectiveness is assessed. Additionally, a comparison of the proposed BSF framework to alternative models is presented.

4.1. Performance Analysis

In this subsection, the accuracy, specificity, precision, sensitivity, and F1 score of the proposed model were assessed. If a patient is healthy, it may be determined using the specificity. As a result, the specificity is established:

$$S = \frac{tn}{tn+fp} \quad (15)$$

The patient's sickness condition is determined by the sensitivity (or recall). By classifying the sample photos detected as true positives in the patients, it is utilised to assess the accuracy of the results. According to estimates,

$$R = \frac{tp}{tp+fn} \quad (16)$$

Where, precision is the characteristic of a successful model prediction and is obtained as,

$$P = \frac{tp}{tp+fp} \quad (17)$$

The representation of real positives and negatives as well as false positives and negatives is measured by the accuracy. It is employed to extract a certain characteristic from photos. The precision is evaluated using,

$$A = \frac{tp+tn}{total\ no.of\ samples} \quad (18)$$

$$F1 = 2\left(\frac{P*R}{P+R}\right) \quad (19)$$

Here, the terms true-positives, true-negatives, false-positives, and false-negatives of the samples are denoted by tp, tn, fp, and fn. The table.1 below displays the model's efficiency.

Table 1. Performance analysis of the proposed method

Class	Specificity	Sensitivity	Precision	F1 score	Accuracy
Saccular aneurysm	99.12	99.04	98.23	99.12	99.80
Mycotic aneurysm	98.20	98.13	97.42	98.74	99.82
Fusiform aneurysm	99.67	99.57	99.76	99.43	99.79

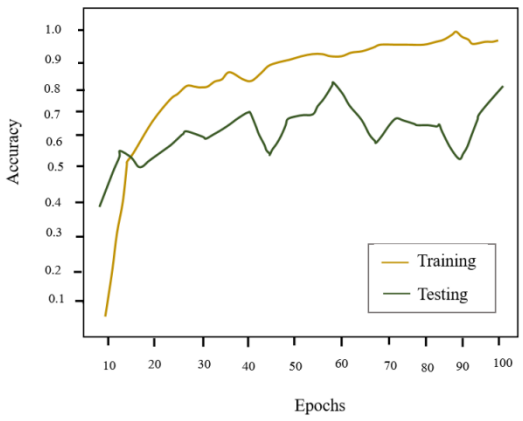

Figure 3. Training and Testing accuracy curve for 3-class classification

The F1 score, specificity, precision, sensitivity, and accuracy were the key characteristics used to evaluate the effectiveness of the suggested BSF framework. Table.1 shows the performance evaluation based on the datasets for the saccular, mycotic, and fusiform classes. The saccular aneurysm (SA), mycotic aneurysm (MA), and fusiform aneurysm (FA) are all accurately identified using this model.

According to the accuracy curve in Fig. 3, which plots accuracy on the y-axis and epochs on the x-axis, the technique's accuracy rises as the number of epochs is increased. The loss of the model diminishes as the number of epochs grows, as seen in Fig. 4's epoch vs loss graph. The BSF model successfully and precisely divides things into three groups

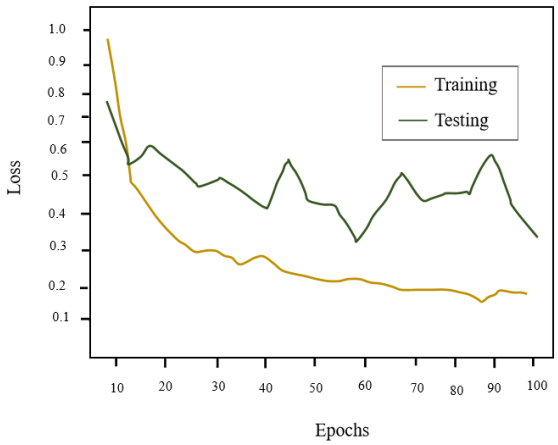

Figure 4. Training and Testing loss curve for 3-class classification

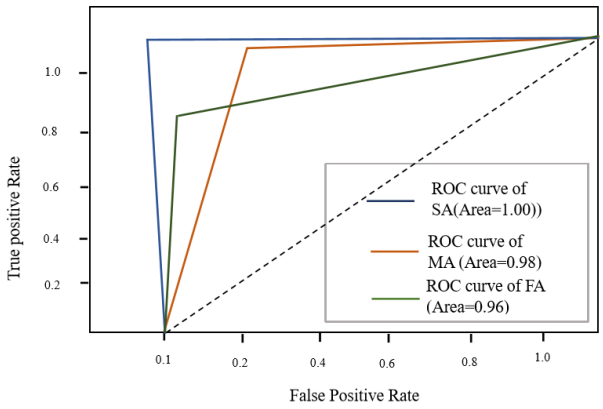

Figure 5. ROC curve for three class classification

Figure 5 shows the ROC calculated for the datasets of MRI images. The TPR and FPR metrics may be used to measure the suggested BSF approach's higher AUC of 0.998 for the 3-class. The suggested model has a 99.80% overall accuracy for three classes.

4.2. Comparative Analysis

In order to confirm that the outcomes of the suggested BSF model attain high accuracy, the effectiveness of each approach was estimated.

The suggested model was evaluated in comparison to four existing approaches, including SVM, CNN, XG Boost, and MRF. The proposed BSF outperformed the other approaches with an accuracy of 99.80%, which was measured using a range of criteria, including specificity,

sensitivity, f1 score, and accuracy. Based on table.2's performance parameters for identifying cervical cancer and obtaining the necessary percentage of classification accuracy, a comparison of several techniques was made. The proposed BSF uses MRI scans to predict brain aneurysms with a total accuracy of 99.80%. However, as compared to the BSF classifier, older methods did not perform as well. In comparison to SVM, CNN, XG Boost, and MRF, the BSF model improves overall accuracy range by 10%, 16.6%, 4.8%, and 0.1%, respectively.

Table 2. Comparison between other methods

Methods	Specificity	Sensitivity	Accuracy
SVM	87.2	88.6	89.8
CNN	84.6	83.8	83.2
XGBoost	94.2	95.8	95.0
Markov Random Field (MRF)	98.8	99.4	99.7
Proposed model	99.2	99.7	99.8

According to the comparison above, the BSF is more accurate than the current models. In order to increase the accuracy of diagnosis, a three-class classification model will be trained in the future. It will properly anticipate the phases of aneurysm. To make the suggested model more useful and practical, it was also trained on data from other areas, such as colposcopy samples. Performance comparison of four classifiers shown in Figure 6.

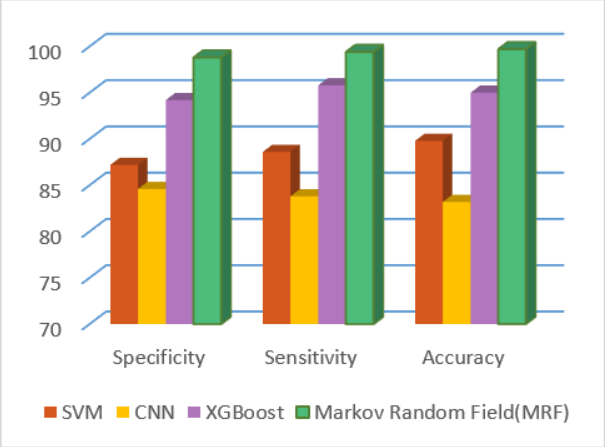

Figure 6. Performance comparison of four classifiers

Table 3. Comparison between proposed and existing models

Year & Author	Model	Accuracy (%)
2023, Xie, Y [9]	SVM	89.8
2023, Ishihara, M [12]	CNN	83.2
2023, Li, X,[14]	XGBOOST	95
2022, Lei, X,[15]	MRF	98.7
Proposed	BSF	99.8

The proposed BSF technique produces results with more accuracy than the cutting-edge approaches, according to the comparison in table.3 above. The suggested BSF model successfully predicts cervical cancer using MRI images with an overall accuracy of 99.8%. However, in comparison to the suggested BSF framework, the current frameworks did not perform well. The suggested model outperforms SVM [9], CNN [12], XGBoost [14] and MRF [15] in terms of overall accuracy by 10%, 16.6%, 4.8%, and 0.1%, respectively. In categorizing the various MRI images, the suggested BSF model outperforms to produce superior classification outcomes.

5. CONCLUSION

This study used MRI scans from IntrA datasets to create a deep learning framework for predicting brain aneurysms. The Kalman filter lowers the distortion noises in the photographs. Therefore, the MRI images are classified using the Spiki Neural Network into saccular aneurysms (SA), mycotic aneurysms (MA), and fusiform aneurysms (FA). Thus, the outcome shows that the suggested method can categorise the MRI images for the purpose of identifying brain aneurysms. The suggested approach outperforms while maintaining a 99.8% accuracy range. Conclusion: The proposed framework outperforms other existing models in terms of accuracy on both training and testing datasets. This method can boost detection rates, enabling quick and accurate clinical treatment.

CONFLICTS OF INTEREST

The authors affirm that they have no known financial or interpersonal conflicts that would have seemed to have an impact on the research presented in this study.

FUNDING STATEMENT

There was no particular grant for this research from any funding organisation in the public, private, or nonprofit sectors.

ACKNOWLEDGEMENTS

The supervisor's guidance and constant support during this research have been much appreciated by the author, who would like to offer his sincere appreciation.

REFERENCES

[1] T.H. Champney, Essential clinical neuroanatomy. John Wiley & Sons. 2023. [CrossRef] [Google Scholar] [Publisher Link]

[2] A. Alaraj, "Virtual reality cerebral aneurysm clipping simulation with real-time haptic feedback", *Neurosurgery*, Vol. 11, No. 1, pp. 52–58, 2015. [CrossRef] [Google Scholar] [Publisher Link]

[3] S.N. Ahmed, and P. Prakasam, A systematic review on intracranial aneurysm and hemorrhage detection using machine learning and deep learning techniques. Progress in Biophysics and Molecular Biology, 2023. [CrossRef] [Google Scholar] [Publisher Link]

[4] B. Kranawetter, M. Hazaymeh, D. Mielke, V. Rohde, and T. Abboud, missing a Blood Blister-Like Aneurysm in the Setting of Aneurysmal Subarachnoid Hemorrhage in a Patient Harboring Multiple Aneurysms. Stroke, 54(9), pp. e434-e437. 2023. [CrossRef] [Google Scholar] [Publisher Link]

[5] T.N. Nguyen, Management of Unruptured Intracranial Aneurysms and Brain Arteriovenous Malformations. CONTINUUM: Lifelong Learning in Neurology, 29(2), pp.584-604, 2023. [CrossRef] [Google Scholar] [Publisher Link]

[6] O. N. Naggara, "Endovascular treatment of intracranial unruptured aneurysms: systematic review and meta-analysis of the literature on safety and efficacy", *Radiology*, vol. 256, pp. 887–897, 2010. [Cross Ref] [Google Scholar] [Publisher Link]

[7] R. S. Bechan, "CT angiography versus 3D rotational angiography in patients with subarachnoid hemorrhage", *Neuroradiology*, vol. 57, pp. 1239–1246, 2015. [CrossRef] [Google Scholar] [Publisher Link]

[8] Y. Xie, "Automatic risk prediction of intracranial aneurysm on CTA image with convolutional neural networks and radiomics analysis", *Frontiers in Neurology*, vol. *14*, 2023. [CrossRef] [Google Scholar] [Publisher Link]

[9] Y. Regaya, "Development of a cerebral aneurysm segmentation method to prevent sentinel hemorrhage", *Network Modeling Analysis in Health Informatics and Bioinformatics*, vol.*12*, no. 1, p.18, 2023. [Cross Ref] [Google Scholar] [Publisher Link]

[10] S. Fujimura, "Development of Machine Learning Model for Selecting the 1st Coil in the Treatment of Cerebral Aneurysms by Coil Embolization", 2023. [Cross Ref] [Google Scholar] [Publisher Link]

[11] M. Ishihara, "Detection of intracranial aneurysms using deep learning-based CAD system: usefulness of the scores of CNN's final layer for distinguishing between aneurysm and infundibular dilatation", *Japanese Journal of Radiology*, vol 41, no. 2, pp.131-141, 2023. [CrossRef] [Google Scholar] [Publisher Link]

[12] A. Niemann, "Deep learning-based semantic vessel graph extraction for intracranial aneurysm rupture risk management". *International Journal of Computer Assisted Radiology and Surgery*, vol. 18, no. 3, pp.517-525, 2023. [Cross Ref] [Google Scholar] [Publisher Link]

[13] X. Li, "Machine learning predicts the risk of hemorrhagic transformation of acute cerebral infarction and in-hospital death". *Computer Methods and Programs in Biomedicine*, vol. *237*, p.107582, 2023. [Cross Ref] [Google Scholar] [Publisher Link]

[14] X. Lei, "Deep Learning-Based Magnetic Resonance Imaging in Diagnosis and Treatment of Intracranial Aneurysm". *Computational and Mathematical Methods in Medicine, 2022*. [Cross Ref] [Google Scholar] [Publisher Link]

[15] B. Wang, "A modified firefly algorithm based on light intensity difference", *Journal of Combinatorial Optimization*, vol. 31, pp.1045-1060, 2016. [CrossRef] [Google Scholar] [Publisher Link]

AUTHORS

A. Jegatheesh received the B.E degree in Electronics and Instrumentation Engineering from Noorul Islam College of Engineering affiliated to Anna University and M.E degree in Applied Electronics from Annna University Regional Campus-Tirunelveli. He received his Ph.D. degree in Information and Communication Engineering from Anna University Chennai, India. Currently he is doing as as an Assistant Professor in Arunachala College of Engineering for Women, Kanyakumari, Tamilnadu. His research area includes Control Systems, Process Control, Image Processing, Signal Processing.

N. Kopperundevi is currently working as Assistant Professor at Vellore Institute of Technology Vellore. She completed her research the year 2019 under Anna University Chennai, in the specialisation of Information Communication Engineering. She has published more than 10 papers and three patents. Acting as a reviewer in Textile Research Journal and Soft Computing has reviewed nearly 10 papers. Her area of interest includes Image Processing, Neural Networks, Fuzzy Systems Machine Learning and Deep Learning and have guided more than 15 UG and PG projects.

M. Anlin Sahaya Infant Tinu is doing her Ph.D research from Anna University, India. She had been working as Assistant professor in A.R. College of Engineering and Maria college of engineering, India. She is now actively doing her research on "Brain Tumor Detection Using Deep Learning Techniques" under the guide ship of Dr. Ahilan Appathurai, Associate Professor in the department of electronics and communication engineering at PSN college of engineering and technology, India. She has attended International Conference on trends in engineering organized by Arunachala College of Engineering for Women, India. She has presented a paper "Automatic Segmentation of Brain Tumor in MRI Images". She also has been a student member of IEEE for three years and actively participated in all the events conducted by IEEE Student Branch-62851.

Arrived: 11.07.2023
Accepted: 19.09.2023